land

MDPI

Article

Impacts of Cropland Utilization Patterns on the Sustainable Use Efficiency of Cropland Based on the Human–Land Perspective

Xinyu Hu [1,2], Chun Dong [2,*] and Yu Zhang [2,*]

[1] School of Geomatics, Liaoning Technical University, Fuxin 123000, China; 47211043@stu.lntu.edu.cn
[2] Chinese Academy of Surveying and Mapping, Beijing 100039, China
* Correspondence: dongchun@casm.ac.cn (C.D.); zhangyu@casm.ac.cn (Y.Z.)

Abstract: Confronted with China's burgeoning population and finite arable land resources, the enhancement of sustainable arable land efficiency is of paramount importance. This study, grounded in the United Nations Sustainable Development Goals (SDGs), introduces a robust framework for assessing sustainable arable land use. Utilizing the Sustainable Utilization of Arable Land (SUA) indicator system, the DGA–Super-SBM model, the Malmquist–Luenberger production index, and the TO–Fisher–OSM algorithm, we evaluated the efficiency of sustainable utilization of arable land (ESUA) in 52 prefecture-level cities within China's major grain-producing regions of the Yellow and Huaihai Seas. We analyzed the cropland utilization patterns from 2010 to 2020, examining the influence of these patterns on sustainable utilization efficiency. Our findings indicate that between 2010 and 2020, the arable land usage in these regions exhibited minimal transformation, primarily shifting towards construction land and conversely from grassland and water systems. Notably, the ESUA of arable land demonstrated an upward trend, characterized by pronounced spatial clustering, enduring high efficiency in the northern regions, and a significant surge in the southern sectors. The declining ESUA (D-ESUA) trend was general but increased in half of the cities. The change in the center of gravity of ESUA correlated with the north–south movement of the proportion of cultivated land area, the turn-in rate, and the turn-out rate, yet moved in the opposite direction to that of cultivated land density and yield per unit area. Variables such as the replanting index, cropland density, yield per unit area, and cropland turn-in rate significantly affected ESUA. These findings offer a scientific basis and decision-making support for optimizing the utilization pattern of arable land and achieving a rational allocation of arable land resources.

Keywords: human–land perspective; sustainable utilization of arable land resources; the main grain-producing areas of the Yellow Huaihai; high-dimensional indicators; impact analysis; SDG

Citation: Hu, X.; Dong, C.; Zhang, Y. Impacts of Cropland Utilization Patterns on the Sustainable Use Efficiency of Cropland Based on the Human–Land Perspective. *Land* **2024**, *13*, 863. https://doi.org/10.3390/land13060863

Academic Editor: Le Yu

Received: 11 May 2024
Revised: 7 June 2024
Accepted: 11 June 2024
Published: 15 June 2024

1. Introduction

Human society is dependent on arable land resources, which directly determine food security and sustainable development [1]. Over recent decades, arable land resources worldwide have experienced severe degradation and decline. The United Nations Food and Agriculture Organization (FAO) estimates that between 1980 and 2018, the world's arable land area shrank by approximately 4% [2]. This decline can be attributed to transitional exploitation and inefficient use of arable land resources, resulting in the deterioration of land quality, ecological degradation, and soil infertility, which limit agricultural production and reduce the ability of humans to address their food needs [3] and run counter to goals such as Zero Hunger and Climate Action, as outlined in the United Nations Sustainable Development Goals (SDGs). China is the largest developing country in the world, accounting for 20% of the world's population; however, only 9% of its land is arable [4]. Protecting China's limited arable land has received significant attention from the Chinese government, who have been establishing a comprehensive set of arable land protection policies and national strategic decisions [5]. However, owing to accelerated urbanization, the expansion

of industrial land, and need for ecological and environmental protection, some of the country's arable land is now being used for other purposes [6]. National Bureau of Statistics data suggest that from 2010 to 2020, China's arable land reduced by approximately 7,533,000 ha, which is approximately the size of the Ningxia Hui Autonomous Region; moreover, the natural ecology around arable land has been affected by the excessive use of chemical fertilizers, pesticides, and agricultural films, leading to low production and inefficient land use. According to the 2020 China Ecological and Environmental Status Bulletin, 19.4% of China's arable land is contaminated; the cost to restore this land would be at least USD 116.3 billion [7]. These facts prompt the need to re-examine China's cropland resource utilization patterns and explore effective ways to improve the efficiency of sustainable utilization of arable land (ESUA) in order to achieve the UN Sustainable Development Goals (SDGs) such as "Zero Hunger", "Climate Action", and "Clean Water and Sanitation" of the UN Sustainable Development Goals (SDGs).

Agricultural land resource utilization is a multifaceted concept that encapsulates the complexities of land planning, distribution, usage, and management. Researchers in this domain are tasked with not only quantifying and qualifying arable land but also assessing the distribution and efficiency of its application. The pattern of cultivated land use encompasses the spatial distribution, quantifiable extent, functional roles, and level of utilization of arable land, among other nuanced characteristics [8]. In the scholarly exploration of agricultural land utilization patterns, domestic and international scholars have expounded extensively on the drivers of land utilization [9], the transformations in land use patterns [10], and the responses to shifts in ecological values [11]. These studies have augmented our comprehension of agricultural land use dynamics. Notably, the analysis of the evolving agricultural land use pattern has been bolstered by the deployment of remote sensing data [12] and socio-economic statistics [13] to delve into the process of land use change [14], its efficiency [13], and its temporal and spatial attributes [15]. These investigations span a spectrum of scales, from the macroscopic intercontinental [11] to the micro-county level [16], offering invaluable insights into the nuances of agricultural land use alterations. In aggregate, the academic discourse on agricultural land use changes has largely focused on the quantity of arable land, shifts in land use patterns, and reactions to ecological value changes, yet it has overlooked the repercussions of land use patterns on the sustainable utilization of agricultural land within the broader context of the United Nations Sustainable Development Goals (SDGs).

The concept of sustainable use was first introduced by the German geographer Hans Carl von Carlowitz in his published work Sylvicultura oeconomica, where he introduced the concept of "Nachhaltigkeit", which states that in the use of resources, not only immediate but also long-term benefits and efficiencies need to be considered to protect the natural environment and socio-economic sustainability. The proposal of sustainable utilization has aroused a strong reaction at the international level. At the 1990 International Symposium on Sustainable Utilization Systems held in New Delhi, India, the concept of sustainable land use was put forward based on the concept of Nachhaltigkeit; at the 1993 Seminar on Sustainable Land Use Management in the 21st Century, held in Canada, the International FAO put forward the "Evaluation Outline of Sustainable Land Management", which set out criteria for the evaluation of sustainable utilization. In-depth studies on the sustainable use of land resources have laid a research foundation and provided models on the sustainable use of cropland, and many studies on the sustainable use of cropland have been carried out worldwide, including those on the theoretical connotations of sustainable cropland use [17,18] and models for sustainable cropland use [19–21]. In 1994, the State Council of China adopted the white paper "China's Agenda 21—Population, Environment and Development", and sustainable development began to involve the field of agriculture. As a major component of agriculture, the sustainable development of arable land has received significant attention. Many subsequent studies have focused on the establishment of indicator evaluation systems and evaluation methods for sustainable use and influencing factors, including the ecological–economic–social model, productive–safety–

protection–economic–social acceptability model, pressure–state–response indicator system, and driving force–pressure-state–impact–response model. There are a range of evaluation methods of sustainable cropland use, including hierarchical analysis, the gray prediction model, coefficient of variation method, multi-factor integrated evaluation method, multiple linear regression model [22], coupled coordination model, structural equation model [23], and ecological footprint model [24], among others. However, most existing research methods and evaluation systems are limited to the statistics and prediction of single system indicators of arable land resources; they cannot meet the comprehensive and accurate evaluation of the sustainable utilization of arable (SUA) land and production efficiency. Moreover, there is a lack of research on the grading of arable land ESUA and the characteristics of the time-space double scale, which is not conducive to the analysis of the SUA evaluation as well as the evolution of the spatial and temporal processes which are even more detrimental to the estimation of the development trend of the sustainable development of arable land.

Considering this context, the present study introduces a comprehensive evaluation framework for the sustainable utilization of arable land, grounded in the United Nations Sustainable Development Goals (SDGs) framework. This framework originates from the interplay between human–land relationships and the balance of inputs and outputs. It constructs an SUA indicator evaluation system that is aligned with the sustainable objectives of production inputs, whilst also encapsulating the economic, social, and ecological expectations, as well as the non-expectations, associated with arable land utilization. Furthermore, the study establishes a sophisticated high-dimensional indicator system evaluation framework that integrates the coupled dimensionally reduced genetic algorithm with the super-efficiency SBM model (DGA–Super-SBM), the Malmquist–Luenberger production index, and the time-sequence optimized optimal segmentation algorithm (TO–Fisher–OSM). This framework is employed to conduct an ESUA evaluation of 52 prefecture-level cities within the major grain-producing regions of the Yellow and Huaihai Seas (YHHRB) in China. Analysis of the shifts in cropland utilization patterns from 2010 to 2020 is conducted, with a keen eye on the essence of cropland utilization patterns. Four key indicators are selected to probe the influence of cropland utilization patterns on the sustainable efficiency of cropland utilization: variations in cropland area, shifts in cropland function, alterations in cropland configuration, and modifications in cropland utilization efficiency. These indicators serve to inform policy makers and provide a robust decision-making tool for the formulation of relevant policies and the sustainable management of cropland resources.

Compared with previous studies, the novelties of this manuscript are centered on three distinct aspects. ① Perspective Innovation. The paper introduces a novel evaluation system for the Sustainable Utilization of Arable land (SUA), drawing upon the United Nations Sustainable Development Goals (SDGs) system. This system is uniquely constructed from the dual vantage points of human–land relationships and the input–output dynamics. Such an approach is unprecedented in the extant scholarly literature, offering a fresh perspective on the assessment of arable land sustainability. ② Methodological Innovation. Leveraging the power of genetic algorithms to optimize a super-efficient Source-Based Model (SBM), this study transcends the limitations of conventional SBM evaluation, which often struggles with high-dimensional parameter spaces. This innovative methodology enables the comprehensive evaluation and analysis of complex, high-dimensional indicator systems. It thus facilitates a profound understanding of the status quo of arable land's sustainable development and promotes the efficient, intensive, and economic utilization of regional arable land. ③ Theoretical Innovation. The paper introduces the concept of cropland utilization patterns, expanding the discourse to encompass four dimensions that influence the ESUA of cropland: area, distribution, function, and utilization degree. This holistic analysis provides a novel theoretical foundation for the sustainable management of cropland resources, offering insights into how these resources can be preserved and utilized for the benefit of future generations.

2. Data and Methods

The comprehensive SUA evaluation system was constructed based on the structure of the economic–social–ecological system (Figure 1). Then, the spatiotemporal evolution of ESUA in the YHHRB was analyzed using DGA–Super-SBM and Malmquist–Luenberger production indices. Finally, ESUA was classified and graded by using TO–Fisher–OSM.

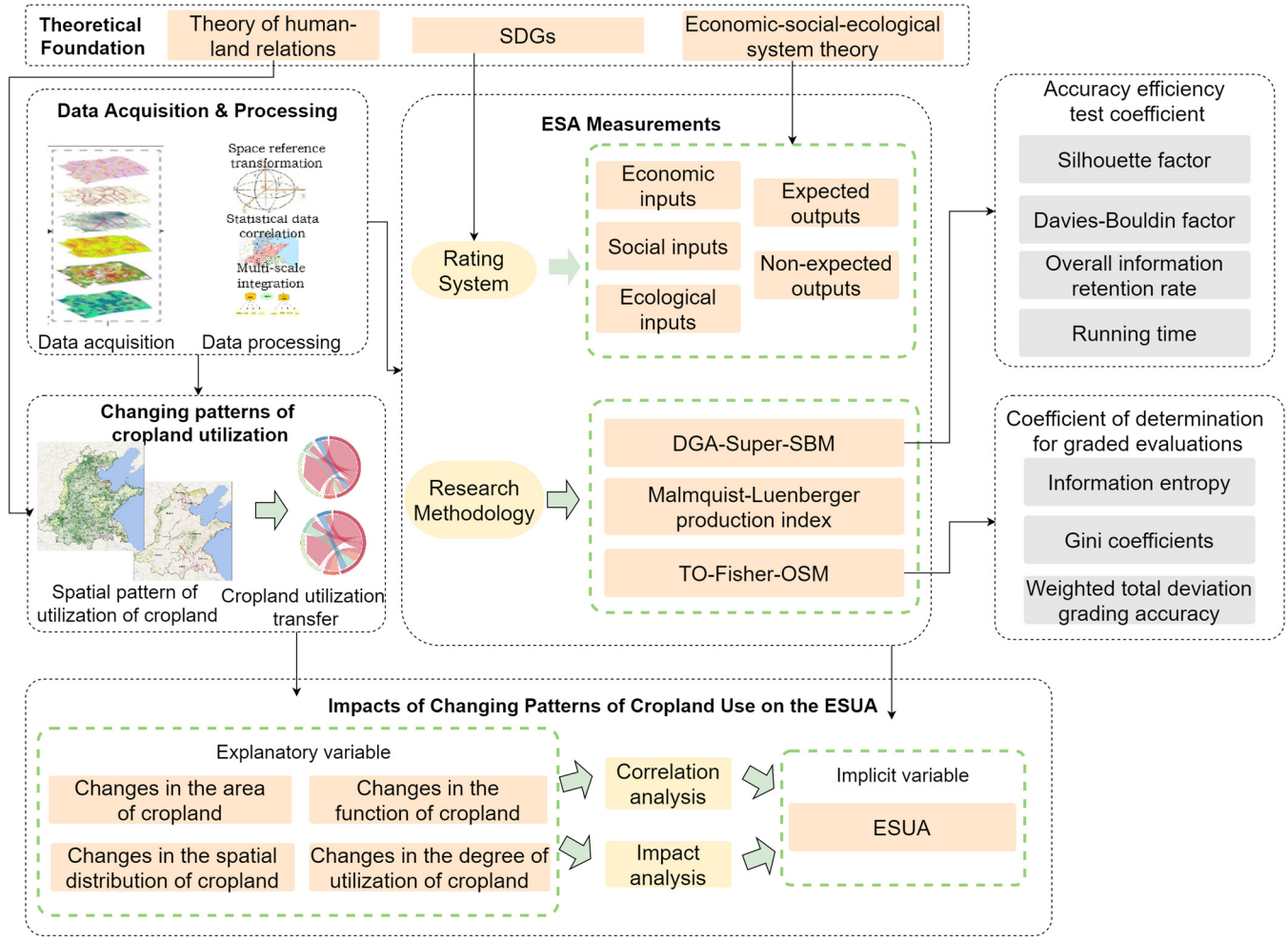

Figure 1. Technology roadmap.

2.1. Conceptual Definition of Cropland Use Patterns

Arable land stands at the heart of agricultural endeavors, shaping a landscape that is decidedly anthropogenic [25]. Subject to immediate human dominion and manipulation, it has evolved in step with the advancement of human civilization. The conceptualization of this vital resource has evolved through the annals of history, its definition broadening to encompass enhanced productivity and innovative land management techniques [26]. Physically, arable land is characterized as a precious terrestrial asset that humanity has reclaimed and put to use to satisfy the demands of life and progress, facilitated by current technological capabilities. It is soil that is hospitable to the growth of crops, endowed with fertility, distinct qualitative attributes, and a favorable soil structure [27].

The utilization pattern of cultivated land encompasses a nuanced and multifaceted construct, spanning the spatial distribution, quantitative dimensions, functionalities, and the degree of utilization of agricultural land, and is a fundamental component of the agricultural production milieu [28]. The spatial distribution of arable land manifests the geographical positioning and extension of this vital resource, serving as a critical determinant that influences the efficiency of arable land utilization and agricultural productivity [29].

The extant area of arable land is intrinsically linked to the scale of food production and the trajectory of agricultural development [30]. The functional evolution of arable land mirrors the diversification of its applications, incorporating multifaceted roles such as food provision, ecological conservation, and recreational tourism [31]. The level of arable land utilization underscores the efficiency and technological sophistication of human utilization, serving as a paramount indicator of the modernization level within agricultural production [32]. Variations in the utilization patterns of cropland encapsulate the alterations in the quantity, location, function, and degree of utilization of cropland across different regions and over temporal intervals. These shifts are contingent upon a multitude of factors, including policy orientation, market demand, technological advancements, and environmental considerations [33]. Consequently, a thorough examination of changes in cropland utilization patterns necessitates an intricate analysis from diverse perspectives. Firstly, the alteration in the acreage of arable land constitutes a pivotal dimension for scrutinizing shifts in the utilization pattern of arable land. An upsurge or decline in arable land acreage reflects the intensity of human engagement with land resources and the scaling of agricultural production. Secondly, the transformation in the function of arable land elucidates the trend toward multifunctionality and the realignment of the agricultural industrial structure. Conversely, modifications in the layout of arable land signal the recalibration of its spatial distribution and the differentiation of agricultural production across regions. Lastly, modifications in the degree of arable land utilization underscore the progression of agricultural production technologies and the enhancement of land resource management methodologies.

2.2. Study Area

The study area was centered on the YHHRB and located between 112°29′ E and the eastern coastline of China and between 31°21′ N and 40°26′ N. This area covers 380,000 km^2 across the middle and lower reaches of the Yellow, Huaihe, and Haihe river basins, including parts of greater Beijing, Tianjin, Hebei, Lu, Henan, northern Jiangsu, and northern Anhui, with a total of 52 prefecture-level municipalities (Figure 2). The area is flat and fertile and covers approximately 32 million ha of arable land, accounting for ~15% of the total arable land in China. The region is rich in water resources, with a number of rivers and lakes providing a solid basis for agricultural production. The area has a warm temperate monsoon climate, four distinct seasons, and average annual sunshine of 1700–2200 h. Due to its special geographic location and the influence of seasonal and climatic factors, the region has fewer hours of sunshine than other parts of China, resulting in a longer crop growth cycle, with most crops maturing twice a year, and some parts of the northern part of the country maturing three times in two years. The main crops include wheat, rice, corn, sorghum, beans, and oilseed, of which wheat and rice are the main food crops. The region is one of the most important food production bases in the country, and plays an important role in the country's economic development and food security.

We chose the YHHRB as a case study for several reasons. First, at the national policy level, achieving food security and sustainability are important concerns, and grain production in the YHHRB is nationally important. Second, natural conditions in the YHHRB are unique, with abundant water resources providing excellent conditions for crop growth. The region has a large amount of high-quality land resources, providing a rich material basis for food production. Cultivated land production conditions are typical of both the North China Plain region and Yangtze River Basin [34], and the study of SUA evaluation in the region can help to provide a reference for cultivated land protection strategies and policies in other key agricultural regions. Third, rapid urbanization in the region has led to a rising demand for land resources. A large amount of arable land has been utilized for production and living purposes, such as industry and urban construction [35], which threatens food security.

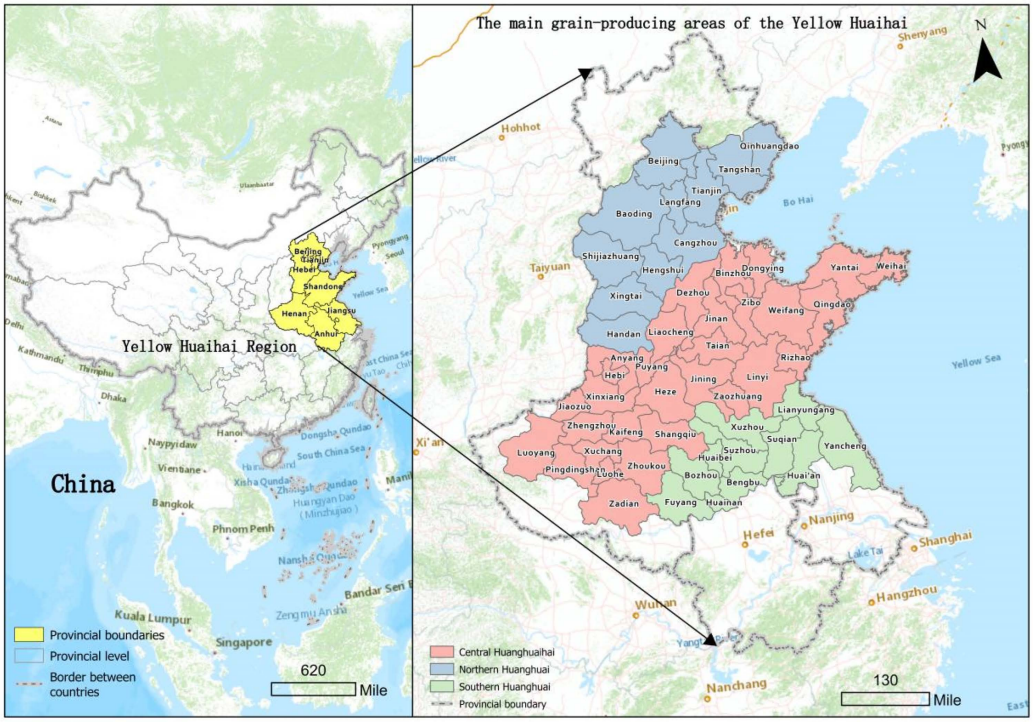

Figure 2. Location map of the project area. Note: This map is based on a standard map [review number GS(2020)4619], retrieved from the Ministry of Natural Resources' standard map service website. The base map is unmodified.

2.3. Research Methods

(1) Calculation of sustainable use efficiency of arable land under high-dimensional indicators using DGA–Super-SBM

Super-SBM is a nonparametric efficiency evaluation method originally proposed by Tone [36]. The model was developed based on the traditional non-expectation SBM model to address input and output slack and directly addresses the problems of excess inputs and insufficient outputs in efficiency assessment. Therefore, Super-SBM is particularly suitable for evaluating ESUA. Recently, Super-SBM has been widely used in the assessment of agro-ecological efficiency and agricultural land use efficiency [37,38]. And in contrast to the conventional CCR model paired with the non-expected SBM framework, the research demonstrates that the super-efficient SBM model exhibits greater precision and trustworthiness. It transcends the constraints encountered by the non-expected SBM model in terms of the scope of its calculated outcomes, thus being able to appraise decision-making units operating at high efficiency levels. However, given that arable land is an intricate and multifaceted ecosystem, a multidimensional indicator system must be considered to assess the sustainable utilization of this resource. Although the super-efficient SBM model has significant utility in evaluating sustainability, the limitations of its modeling parameters can introduce distortions when computing within the context of a high-dimensional indicator system within the super-efficient SBM model. Genetic algorithm-based dimensionality reduction involves the mapping of high-dimensional data into a lower-dimensional space. Unlike conventional dimensionality reduction techniques, such as principal component analysis (PCA) [39], genetic algorithms have the capacity to select a superior projection matrix, thereby more effectively preserving the structural integrity of the original data. Consequently, this study employs an SBM model coupled with a genetic algorithm for dimensionality reduction to evaluate the sustainable efficiency of arable land resource use.

The detailed calculation process of the Super-SBM model is described in the literature. In brief, the Super-SBM model contains non-desired outputs as follows:

$$\min\rho = \frac{\frac{1}{m}\sum_{i=1}^{m} s_i^- / x_{in}}{1+\frac{1}{s_{1+s_2}}\left(\sum_{r=1}^{s_1} s_r^g / y_{rn}^g + \sum_{l=1}^{s_2} s_l^b / y_{ln}^b\right)} \quad (1)$$

where ρ is the target efficiency value, s^- is the amount of slack in the input schedule, s^g is the amount of slack in the desired output, and s^b is the amount of slack in the undesired output.

(2) Calculation of Dynamic sustainable efficiency of cropland (D-ESUA) through the Malmquist–Luenberger Production Index

As the technical efficiency of DGA–Super-SBM assessment is based on 1 year of data, it is suitable for dealing with static changes in ESUA [40]. In analyzing the SUA state, the initial state of utilization changes from period to period, and the conditions under which the ESUA is analyzed are different in each case. For this reason, when calculating ESUA, scholars have proposed evaluation methods that can be compared over time [41]. The dynamic Malmquist production index is based on a distance function to analyze the efficiency changes and technical progress of decision-making units [42–44].

As the traditional Malmquist index ignores the constraints of environment and resources, combined with the actual situation of the YHHRB, in this study, we adopted the Malmquist–Luenberger production index based on the directional distance function of SBM, which is able to analyze the dynamic change of the efficiency of cultivated land use, and to identify how to improve the desired output and reduce pollutant emissions based on the integrated cultivated land and external environmental factors. The Malmquist–Luenberger production index formula is as follows:

$$ML_t^{t+1} = \left[\frac{1+\vec{D}_0^t(x^t, y^t, z^t; y^t, -z^t)}{1+\vec{D}_0^t(x^{t+1}, y^{t+1}, z^{t+1}; y^{t+1}, -z^{t+1})} \times \frac{1+\vec{D}_0^{t+1}(x^t, y^t, z^t; y^t, -z^t)}{1+\vec{D}_0^{t+1}(x^{t+1}, y^{t+1}, z^{t+1}; y^{t+1}, -z^{t+1})}\right]^{1/2} \quad (2)$$

where ML_t^{t+1} is the index of change in production, $\vec{D}_0^t(x^t, y^t, z^t; y^t, -z^t)$ and $\vec{D}_0^t(x^{t+1}, y^{t+1}, z^{t+1}; y^{t+1}, -z^{t+1})$ are the technology in period t as the reference technology (distance functions for decision units in periods t and $t+1$), and $\vec{D}_0^{t+1}(x^t, y^t, z^t; y^t, -z^t)$ and $\vec{D}_0^{t+1}(x^{t+1}, y^{t+1}, z^{t+1}; y^{t+1}, -z^{t+1})$ are the technology of period $t+1$ as the reference technology (distance function of the decision unit in period t and period $t+1$).

(3) Classification of ESUAs using TO–Fisher–OSM

Fisher's optimal partitioning method is an ordered clustering algorithm first proposed by the British statistician Ronald Fisher in 1958; the purpose of the algorithm is to find an optimal solution that makes the solution of each sub-problem optimal, so as to obtain the optimal solution of the original problem. Fisher's optimal partitioning method has been widely applied in the field of agriculture, and is used to assess the efficiency of agricultural production and land use, including the efficiency of agricultural resource utilization [45], crop growth detection [46], cropland potential assessment [47], and land quality analysis [48], among others. The traditional optimal segmentation algorithm can only obtain a local optimal solution rather than a global optimal solution, owing to the limitation of the local optimal solution, and is only applicable to short time-series and small-scale data; the computation amount and time increase exponentially for long time-series and large-scale data [49]. Therefore, in practical application, the traditional optimal segmentation method cannot meet the hierarchical division of ESUA in the study area. The manipulation of extensive long-term time-series data remains an underdeveloped area of research. Nonetheless, the processing of time-series data is integral to the examination of the sustainable dynamics of arable land. Consequently, this paper integrates Principal Component Analysis (PCA) with Fisher's Optimal Segmentation Method (FOSM) to create

the TO–Fisher–OSM model, thereby enhancing its proficiency in handling time-series data. Compared with the commonly used natural breakpoint method, it can effectively segment the series in time and space through mathematical models and algorithms, and can adaptively select appropriate segmentation algorithms according to the characteristics of different series [50]. TO–Fisher–OSM can select the components that best cover the characteristics of the original data as principal components to complete the dimensionality reduction of the time series and serve as categorical variables, and can use as few principal components as possible to express the variability of the data, which not only reduces the number of categorical variables, but also better captures the correlation between the variables so as to improve the accuracy of the model. Its principle is as follows:

$$\begin{cases} L[P(n,2)] = \min_{2\le j\le n} D(1,j-1) + D(j,n), \\ L[P(n,k)] = \min_{k\le j\le n} \{L[P(n,k)] + D(j,n)\} \end{cases} \quad (3)$$

where n is the sample size, k is the number of splits, b(n, k) is the sample size split into k classes, D(i, j) is the sum of the squares of the deviations, L(i, j) the loss function, and P(n, k) is the minimum of L[P(n, k)], namely $L[P(n,k)] = \min_{1=i_1<i_2<i_g<\cdots<i_k<i_{k+1}=n+1} L[b(n,k)]$.

2.4. SUA Evaluation System Construction

Drawing upon the United Nations Sustainable Development Goals (SDGs) as a framework, this paper references the National Sustainable Agricultural Development Plan (2015~2030) and builds upon the findings of prior research [23,51]. Additionally, considering the regional peculiarities of the YHHRB, and adhering to the principles of systematicity, representativeness, and utility, a comprehensive evaluation system for Sustainable Agricultural (SUA) has been constructed, encompassing economic, social, and ecological dimensions. In total, 23 indicators, including film inputs, machinery inputs, and light inputs, were selected as input indicators; six indicators (arable land value per capita, number of employees in agriculture, forestry, animal husbandry, and fisheries, and sewage treatment rate) were selected as desired output indicators; three indicators (carbon emissions, surface pollution in agriculture, and the intensity of the grey-water footprint of the plantation industry) were selected as non-desired output indicators. The accessibility and operability of the index data were considered, and the comprehensive evaluation system for the sustainable utilization of YHHRB cropland was finally established as shown in Table 1.

Table 1. YHHRB comprehensive evaluation system for sustainable utilization of cultivated land.

System of Indicators	Initial Indicators	Secondary Indicators	Tertiary Indicators	Unit
SUA evaluation system	Economic inputs	Film inputs	Agricultural plastic film use per unit of GDP	t/CNY 1 million
		Fertilizer inputs	Fertilizer application per unit of GDP	t/CNY 1 million
		Pesticide inputs	Pesticide use per unit of GDP	t/CNY 1 million
		Government inputs	Percentage of expenditure on agriculture	%
		Electricity inputs	Rural electricity consumption	KWh
	Social inputs	Labor inputs	Size of rural population	%
			Ease of farming	km
			Cultivated land area per capita	ha/per
			Rotation and fallow status	%
		Mechanized inputs	Degree of agricultural mechanization	kilowatt
		Irrigation inputs	Effective irrigated area	Kha
			Distance to water source	km

Table 1. *Cont.*

System of Indicators	Initial Indicators	Secondary Indicators	Tertiary Indicators	Unit
SUA evaluation system	Ecological inputs	Land inputs	Cropland fragmentation	Blocks/Kha
			Percentage of high-grade arable land	%
			Share of arable land area	%
			Cropland type as a percentage	%
			Percentage of basic farmland area	%
		Resource inputs	Percentage of area graded by slope	%
			NDVI	
			Soil-water harmony	m^3/ha
			Ratio of cropland area to forest and grassland area	
		Light input	Length of exposure	Hour
	Expected outputs	Economic benefits	Value of arable land per capita	CNY/per ten thousand CNY
			Disposable income per rural household	
			Value of ecological services	ten thousand CNY
		Social benefits	Coefficient of income disparity between urban and rural areas	
			Production per unit area of arable land	t/ha
		Ecological benefit	Percentage of forest cover	%
			Sewage treatment rate	%
	Unexpected outputs	Gaseous waste	Carbon footprint	mt
		Solid waste	Agricultural surface pollution	t
		Liquid waste	Graywater footprint intensity of cultivation	m^3/kg

2.5. Data Sources

This study used panel data from 52 prefecture-level cities in the YHHRB from 2010 to 2020. The resources used to compile panel data for the 52 prefecture-level cities from 2011 to 2021 included the China Urban Statistical Yearbook, China Regional Economic Statistical Yearbook, Hebei Statistical Yearbook, Jiangsu Statistical Yearbook, and Third National Land Survey databases; some missing data were supplemented by interpolation or exponential smoothing. Owing to the different positive and negative directions and unit magnitudes of the data for each indicator, it was necessary to standardize the original data using the positive indicator standardization Formula (4) and negative indicator standardization Formula (5) before performing data calculation:

$$b_{ij} = \frac{a_{ij} - a_j^{min}}{a_j^{max} - a_j^{min}} \quad (4)$$

$$b_{ij} = \frac{a_j^{max} - a_{ij}}{a_j^{max} - a_j^{min}} \quad (5)$$

where b_{ij} is the normalized value, a_{ij} is the ith value of the j metrics, and a_j^{max} and a_j^{min} are the maximum and minimum values of the j indicators, respectively.

3. Results and Analysis

3.1. Changing Patterns of Cropland Use

The utilization patterns of arable land in the YHHRB over the period from 2010 to 2020 are delineated in Table 2 and Figure 3. Scrutiny of the temporal aspect reveals that between 2010 and 2015, the allocation of arable land exhibited minimal fluctuation, with a staggering 96% of the arable land within the municipal jurisdiction remaining unaltered. The prevalent outward movement of arable land was toward conversion into construction land, whereas the principal inward movement stemmed from the transformation of grassland. Notably, the extent of arable land ceding from the region between 2015 and 2020 was marginally reduced by 1.1%, registering a general trend of stability. The quantum of land transitioning to construction purposes diminished by a significant 35.41%, whereas there was a discernible upsurge of 15.7% in the conversion of land to shrubbery. The reversion of grassland and forested areas to arable land collectively accounted for 71.2% of the total area subjected to conversion. These findings suggest that throughout the trajectory of arable land conversion, there is a palpable diminution in the expanse of non-agricultural territories, such as construction land and shrub land, concurrent with a gradual expansion of the agricultural landmass.

Table 2. Arable land use transfer matrix, 2010–2020.

2010–2020	Grassland	Cropland	Dioecious	Wasteland	Building Land	Woodland	Wetlands	Water
grassland	33,594.14	4122.92	213.50	38.78	325.30	2331.10	0.01	35.41
cropland	2838.78	1,004,189.64	1.49	2.56	24,753.50	4107.92	0.01	3351.35
dioecious	272.50	3.28	1241.82	0.00	0.02	243.19	0.00	0.00
wasteland	17.62	137.31	0.00	2507.44	1051.03	0.00	0.00	1293.35
building land	0.18	20.75	0.00	1.16	268,226.19	0.04	0.00	1333.50
woodland	15.85	3499.95	344.19	0.00	142.99	125,633.98	0.00	0.86
wetlands	0.00	0.00	0.00	0.00	0.00	0.00	0.00	0.00
water	5.75	3798.17	0.00	355.58	2205.81	9.77	0.00	37,635.35

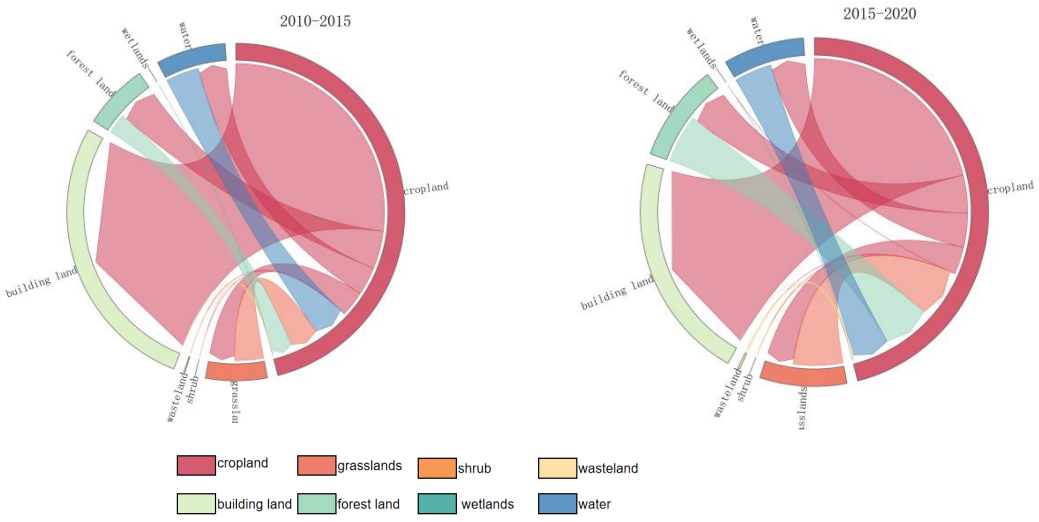

Figure 3. Arable land use transfer chord, 2000–2020.

Spatially, the interconversion of arable land and other land types within the YHHRB exhibits pronounced spatial heterogeneity (Figure 4). The primary sources of arable land conversion in these areas are grassland, aquatic systems, and forested land. The reclamation of grassland is particularly prevalent in the western reaches of Hebei Province, the central and southern districts of Shandong Province, and the western portion of Henan Province, with grassland contributing to 35.59% of the converted arable land. Aquatic systems are the

source of 32.79% of the converted arable land, primarily located in the eastern and southern parts of Jiangsu Province, the central region of Tianjin, and the southeastern portion of Anhui Province. Forested land accounts for 30.21% of the converted arable land, primarily distributed across Beijing, Henan Province, and Hebei Province. The transfer of grassland and aquatic systems exhibits a pattern of spatial clustering, whereas the distribution of forested land is more diffuse. Arable land is primarily acquired from construction land and forested land, with the area of arable land transferred to construction land representing 70.61% of the total converted area, primarily occurring in Anhui Province, Hebei Province, and the Municipality of Tianjin. The area transferred to forested land constitutes 11.72% of the converted area, primarily found in the Municipality of Beijing, Jiangsu Province, and Shandong Province.

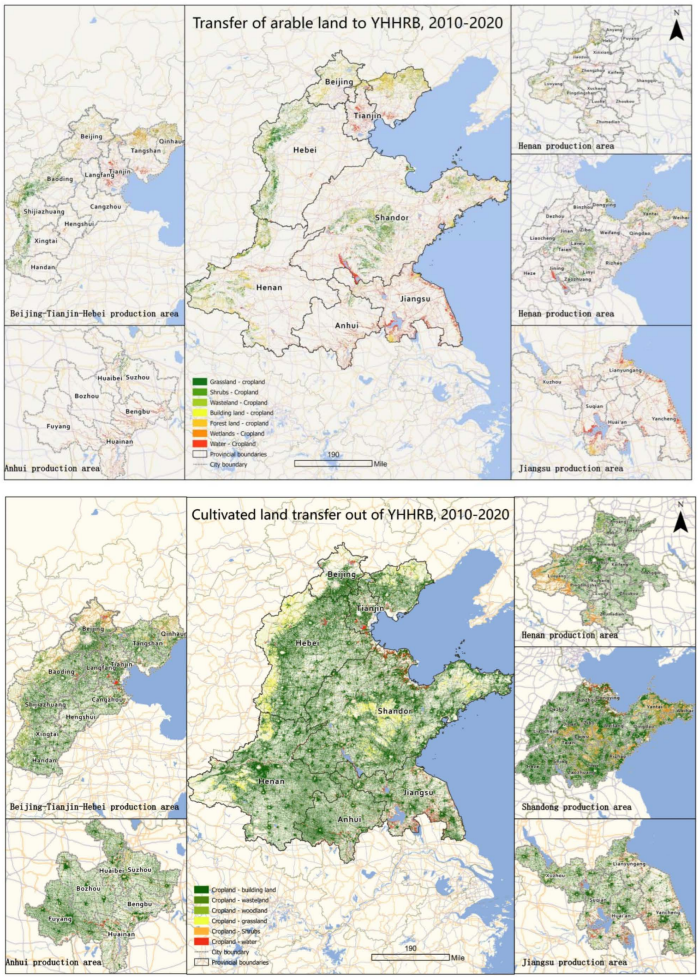

Figure 4. Spatial pattern of changes in cropland use, 2010–2020.

3.2. Characterization of the Spatial and Temporal Evolution of the Efficiency of the Sustainable Use of Arable Land

3.2.1. Model Optimization Evaluation

In this study, the Super-SBM, DGA–Super-SBM, and projection-seeking model for evaluating high-dimensional indicators were compared in terms of model performance by being used to evaluate the SUA land resources in a high-dimensional indicator system. In evaluating model performances, we adopted five indicators: the silhouette coefficient, Davies–Bouldin index, overall information retention rate, running time, and visualization test. The silhouette coefficient measures the tightness within the cluster to which each sample belongs and the separation from other clusters. Higher silhouette factors indicate a better distribution of samples and a more accurate delineation of clusters. The Davies–

Bouldin index measures the similarity between coarseness and the closeness within clusters. A lower Davies–Bouldin index indicates a better delineation of clusters. The combined assessment of these two metrics was used to reflect the modeling performances of the three models. The overall information retention rate measures the amount of information retained in the downscaled dataset relative to the original dataset, and the expectation is that the downscaled dataset will retain sufficient information while reducing dimensionality to maintain model accuracy and evaluative power. Running time can directly affect model efficiency and practicality in practical applications. The calculation results of the above four indicators are shown in Table 3. Finally, the three models were visualized and examined by scatter plots, and the distribution and clustering of the dimensionality-reduced data and original data were observed to determine whether the dimensionality-reduced data could effectively express the structure of the original dataset (Figure 5). We found that DGA–Super-SBM was the most suitable model for evaluating the SUA of land resources.

Table 3. Model performance evaluation.

Norm / Model	Silhouette Factor	Davies–Bouldin Index	Overall Information Retention Rate	Running Time
Super-SBM	0.5779	0.4229	—	2s'26
DGA–Super-SBM	0.7604	0.3023	94.96%	0s'91
Projective tracing algorithm	0.5816	0.4819	11.44%	3s'81

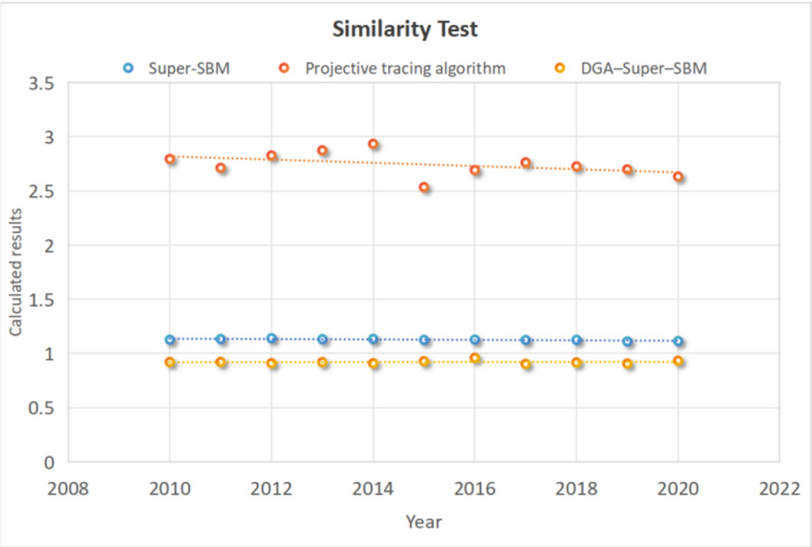

Figure 5. Similarity tests. Note: In the figure, the trend and the amount of information of DGA–Super-SBM and Super-SBM are basically kept the same, while the difference of Projective tracing algorithm is larger.

3.2.2. Characterization of the Time Evolution of Sustainable Use Efficiency of Arable Land

In this study, based on the national strategy of sustainable development of food production, the YHHRB was divided into seven regions according to administrative districts (Table 4). The average value of ESUA of arable land from 2010 to 2020 was calculated on the basis of administrative regions (Figure 6).

Table 4. Yellow–Huai–Hai River Basin (YHHRB) regional divisions.

Administrative Divisions	Province	Prefecture-Level City
Northern YHHRB	Beijing Tianjin Hebei	Shijiazhuang, Qinhuangdao, Tangshan, Langfang, Baoding, Cangzhou, Hengshui, Xingtai, Handan
Central YHHRB	Shandong	Jinan, Dezhou, Binzhou, Dongying, Zibo, Weifang, Yantai, Weihai, Liaocheng, Qingdao, Heze, Jining, Zaozhuang, Linyi, Rizhao, Tai'an
	Henan	Zhengzhou, Anyang, Puyang, Hebi, Xinxiang, Jiaozuo, Luoyang, Kaifeng, Shangqiu, Xuchang, Pingdingshan, Luohe, Zhoukou, Zhumadian
Southern YHHRB	Anhui Jiangsu	Huabei, Bozhou, Cebu, Fuyang, Bengbu, Huainan Xuzhou, Lianyungang, Suqian, Huai'an, Yancheng

Figure 6. ESUA distribution in the Yellow–Huai–Hai River Basin.

From Figure 6, from 2010 to 2020, 44.23% of cities in the YHHRB had arable land with ESUA of >1. Among them, Beijing had the largest value (1.3727), followed by Cangzhou City (1.1347); the lowest value is for Hebi City (0.4717). Overall, the average ESUA value for the YHHRB from 2010 to 2020 was 0.9012, and the number of more efficient and efficient cities increased from 15.38% in 2010 to 23.07% in 2020; the number of cities with medium efficiency or above decreased from 67.31% in 2010 to 71.15% in 2020, indicating that the region as a whole increased from low efficiency to medium efficiency. Figure 5 also shows regional differences in ESUA. At the provincial level, 11.54% of cities in Hebei Province had an ESUA of >1, 7.69% of cities in Henan Province had an ESUA of >1, 5.77% of cities in Jiangsu Province had an ESUA of >1, 13.46% of cities in Shandong Province had an ESUA of >1, and 1.92% of cities in Anhui Province had an ESUA of >1. Except for Beijing

and Tianjin, the two municipalities with the highest efficiency, the ESUA of the remaining provinces was in the order of Hebei > Jiangsu > Shandong> Henan > Anhui.

Figure 7 shows temporal changes in ESUA. ESUA for the whole YHHRB showed an increasing and then decreasing trend, with ESUA peaking in 2016 and decreasing from 2016 to 2020. ESUA in the northern YHHRB consistently maintained a high efficiency level during the study period, with a mean value of 1.136. The gap between ESUAs in the central and northern regions gradually narrowed, with a mean value of 0.866; in the southern region, ESUA had a clear upward trend, with a mean value is 0.878. The results show that ESUA is more efficient in the northern part of the YHHRB than in the central and southern parts. In the YHHRB, land management policies as well as high-tech agricultural development strategies are relatively developed in the northern region, where local governments utilize advanced high-tech agricultural applications and environmental protection to spend more resources on improving ESUA [52]. The central region has rich land resources and has experienced sustainable and efficient development of arable land; however, owing to poor agricultural management, a large amount of reclaimed arable land has had a decline in stability and quality, leading to a decline in the ESUA [14]. Although ESUA in the southern region was lower than that in the northern and central provinces in 2010, its favorable geographical location and land resources, coupled with a push to develop green agriculture and increase investment in agricultural science and technology, have allowed the ESUA to gradually improve, contributing to a steady increase in the efficiency of cultivated land in the YHHRB in terms of sustainability.

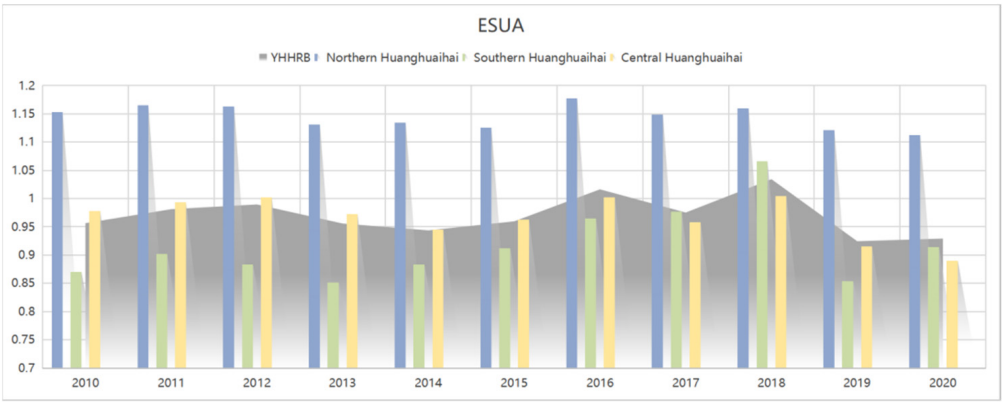

Figure 7. Temporal changes in average ESUA in different regions of the YHHRB.

3.2.3. ESUA Spatial Difference Characterization

We named the evaluation efficiency of the sustainable use of arable land from low to high as the low efficiency zone, lower efficiency zone, medium efficiency zone, higher efficiency zone, and high efficiency zone, and from Figure 6, we can see that there are 30 cities, accounting for 57.7%, in the high efficiency zone and higher efficiency zone, and 10 cities, accounting for 19.23%, in the medium efficiency zone, so it can be seen that the Huanghuaihai region as a whole is in a higher sustainable use efficiency level. From Figure 6, ESUA in the YHHRB increases from west to east, and spatial agglomeration is obvious. The overall high ESUA in the northeast and low ESUA in the southwest are mainly due to differences in the (1) soil and water resources, (2) the level of agricultural science and technology, and (3) land occupation and environmental pollution. First, the northeastern YHHRB is mostly plains, with fertile soil, sufficient water sources, and flat terrain; in contrast, the southwestern YHHRB is mostly mountainous and hilly, with overall poor land quality, shallow soils, low soil fertility, and severe soil erosion, all of which restrict arable land use [53]. Second, the northeastern region of the YHHRB, which has a more advanced economy and level of development, has a much higher level of agricultural mechanization and agricultural science and technology input than the southwestern region; larger government investment in agriculture is indispensable to rapidly improving ESUA [54]. Finally, the southwestern

region of the YHHRB suffers from poor land development and environmental pollution caused by urban expansion and industrial development, which has greatly limited the ESUA of local arable land. Supporting the sustainable development of arable land requires increased land governance and environmental protection [55].

3.2.4. Dynamic Sustainable Efficiency of Cropland

Figure 8 shows changes in 2-yearly ESUA data for each province in the YHHRB from 2010 to 2020. We observed a negative overall change in D-ESUA (0.9977) over the research period, with D-ESUA decreasing by 2.3% per year. The average sustainable efficiency of cropland resources from 2010 to 2020 showed a fluctuating trend, indicating that SUA in the YHHRB is still in the exploratory development stage. The number of provinces showing a positive offset (>1) in D-ESUA during the study period accounted for 50% of the entire YHHRB, among which Beijing and Tianjin had the highest average annual growth rates (4.89 and 5.56%, respectively). While the other provinces did not show an offset in efficiency, they also showed an increasing trend yearly. In summary, according to D-ESUA analysis, the YHHRB is still in the exploratory stage in terms of sustainable development of arable land, but it is expected to experience rapid development in the near future.

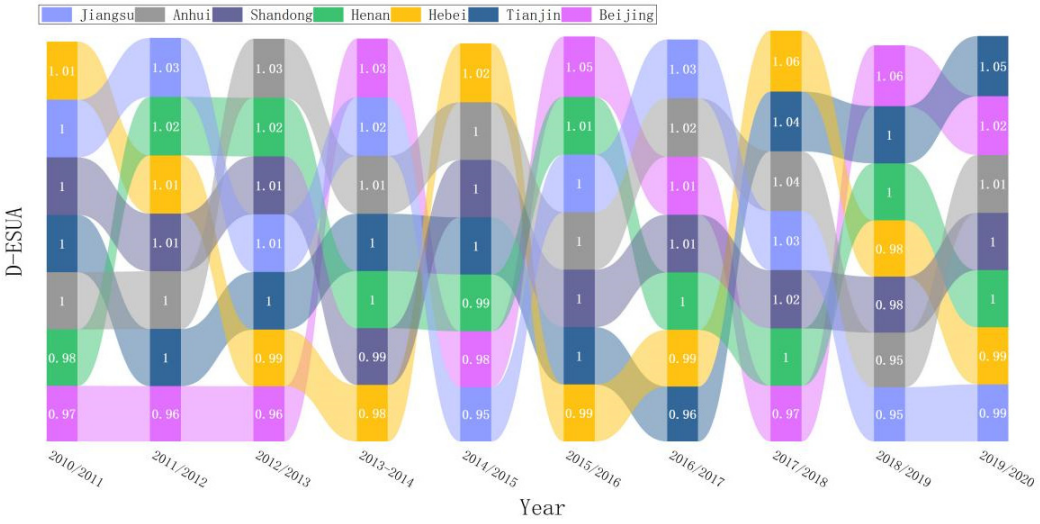

Figure 8. Temporal changes in dynamic sustainable efficiency of cropland for different provinces of the YHHRB.

Figure 9 shows average D-ESUA values for different regions over time. The D-ESUA of the whole YHHRB fluctuated between 2010/2011 and 2017/2018; between 2017/2018 and 2019/2020, it decreased and then increased. D-ESUA values were highest in the southern region from 2010/2011 to 2013/14 and in 2016/2017; they were highest in the northern region from 2014/2015 to 2019/2020 (with the exception of 2016/17). During the study period, D-ESUA in the northern region increased from low to high efficiency, probably owing to local government policies on arable land protection and the rapid development of new agricultural technologies. D-ESUA resources in the central and southern regions were slow to improve, experiencing a fluctuating rising trend, probably because of the transition of land cultivation due to local climate and crop maturity, which led to a decline in land quality and affected the sustainable development efficiency of arable land.

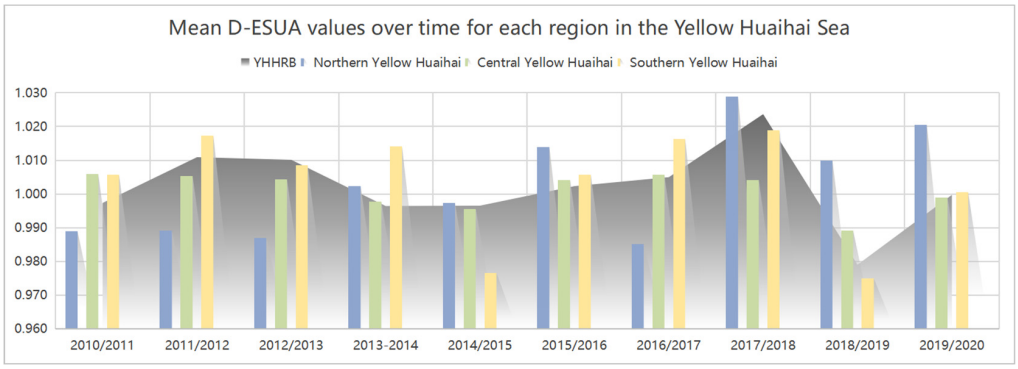

Figure 9. Temporal changes in mean dynamic sustainable efficiency of cropland (D-ESUA) for each region of the Yellow–Huai–Hai River Basin (YHHRB).

3.2.5. Grading of the Efficiency of the Sustainable Use of Arable Land

We used the natural breakpoint, optimal segmentation, and TO–Fisher–OSM methods to classify the SUA of land, to explore the most suitable classification model for SUA in the YHHRB. The natural breakpoint method is automatically generated by ArcGIS; the results of the optimal segmentation method and TO–Fisher–OSM are shown in the following Tables 5 and 6, respectively. According to the actual needs of arable land classification, we set the number of classification to five.

Table 5. Grade classification based on the optimal partitioning method.

Number of Categories	Error Function	Optimal Segmentation Results
2	0.3788	1–15,16–54
3	0.2296	1–3, 4–15, 16–54
4	0.1329	1–3, 4–15, 16–50, 51–54
5	**0.0724**	**1, 2–6, 7–15, 16–50, 51–54**
6	0.049	1, 2–5, 6–11, 12–15, 16–50, 51–54
7	0.0278	1, 2–5, 6–11, 12–15, 16–43, 44–52, 53–54
8	0.0189	1, 2–5, 6–11, 12–15, 16–39, 40–48, 49–52, 53–54
9	0.0128	1, 2–3, 4–6, 7–11, 12–15, 16–39, 40–48, 49–52, 53–54
10	0.0095	1, 2–3, 4–6, 7–11, 12–15, 16–24, 25–41, 42–49, 50–52, 53–54

Note: The color-emphasized fonts in the table are the optimal solutions of the Optimal Segmentation and TO-Fisher-OSM algorithms chosen by the authors.

Table 6. Grade classification based on the TO–Fisher–OSM method.

Number of Categories	Error Function	TO–Fisher–OSM Results
2	0.6249	1–15, 16–54
3	0.3066	1–15, 16–52, 53–54
4	0.1513	1–12, 13–23, 24–52, 53–54
5	**0.0931**	**1–3, 4–12, 13–23, 24–52, 53–54**
6	0.0552	1–3, 4–12, 13–19, 20–38, 39–52, 53–54
7	0.039	1–3, 4–12, 13–17, 18–23, 24–45, 46–52, 53–54
8	0.0293	1–3, 4–12, 13–17, 18–23, 24–36, 37–48, 49–52, 53–54
9	0.0226	1–2, 3–9, 10–12, 13–17, 18–23, 24–36, 37–48, 49–52, 53–54
10	0.0168	1–2, 3–9, 10–12, 13–15, 16–19, 20–23, 24–36, 37–48, 49–52, 53–54

Note: The color-emphasized fonts in the table are the optimal solutions of the Optimal Segmentation and TO-Fisher-OSM algorithms chosen by the authors.

Maintaining the main statistical characteristics of data is an important principle in data classification. There are three commonly used grading evaluation models: information entropy, the Gini coefficient, and weighted total deviation grading accuracy evaluation model. Information entropy measures a dataset's existence, focusing on measuring information uncertainty; the smaller the information entropy, the more reasonable the division. The Gini

coefficient is used to extract the Gini impurity to measure the uncertainty or impurity of the rank classification; the smaller the Gini coefficient, the more reasonable the classification. The weighted total deviation grading accuracy model considers the consistency within and between grades and focuses on the evaluation of the grading interval; the closer the grading accuracy model is to 1, the better the model performance. The three evaluation models only consider one or two factors that affect the merits of grading, and do not have universality for all grading results; therefore, they have greater limitations in practical application.

To evaluate the grading results more comprehensively, we comprehensively considered these three evaluation models as the attributes of multi-attribute decision making, that is, as evaluation indices for determining the reasonableness of grading based on the natural breakpoint method, optimal segmentation method, and TO–Fisher–OSM method (Table 7, Figure 10). There were large differences in grading among the three grading methods, with TO–Fisher–OSM offering the best grading accuracy and reasonableness. From Figure 10, the natural breakpoint approach provided good grading visually and a more uniform distribution at all levels; however, the demarcation points did not completely show the data distribution features. The optimal segmentation method emphasized data distribution features; however, there was some data aggregation, and the data distribution at all levels was unequal, obscuring the spatial rank inequalities in the YHHRB. TO–Fisher–OSM could fully highlight the data distribution characteristics while maintaining the overall sense of balance, quantity, and rank of SUA in the YHHRB. Moreover, the visualization effect was better than that of the other methods.

Table 7. Determination of grading evaluation results.

	Information Entropy	Gini Coefficient	Weighted Total Deviation Grading Accuracy
Natural breakpoint method	0.6448	0.1082	0.1805
Optimal segmentation method	0.4945	0.1176	0.1829
TO–Fisher–OSM	0.3987	0.0660	0.4247

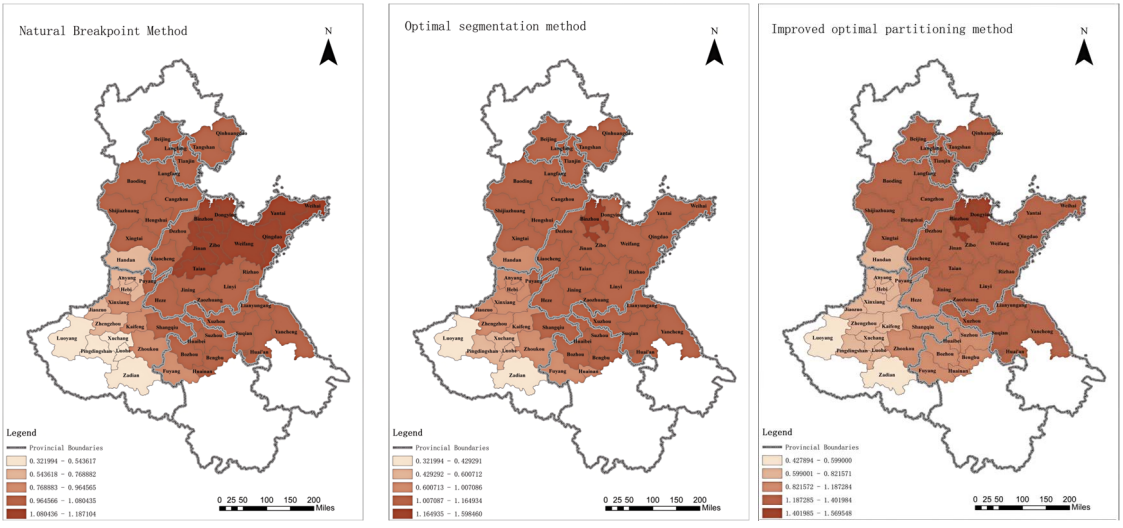

Figure 10. Thematic diagrams of ESUA grade classification.

3.3. Analysis of the Correlation between Changes in Cropland Use Patterns and Sustainable Use Efficiency of Cropland

This investigation isolates variables from four distinct dimensions: arable land area, arable land function, arable land configuration, and arable land utilization intensity. These dimensions are examined to discern the repercussions of alterations in the structure of arable land use on the efficiency of its sustainable utilization. The core indicators encompass

① Arable Land Area Ratio, which quantifies the retention of arable land within the YHHRB by comparing the regional arable land area to the total regional area; ② cultivated land transfer rate, signifying the proportion of land area that transitions from alternative land use categories to arable land; ③ cropland turnover rate, indicating the proportion of land area that converts from arable land to other land use types; ④ Arable Land Shape Index, which evaluates the degree of clustering or dispersal of arable land by assessing the deviation of the regional arable land form from a circular or square shape of equivalent area; ⑤ Arable Land Density, which assesses the clustering of arable land by calculating the number of arable land patches per unit of area; ⑥ Yield per Unit Area, representing the productivity of arable land, or the quantity of foodstuffs yielded per unit of arable land area; ⑦ Arable Land Replanting Index, reflecting the extent of arable land utilization within a given area, computed by the ratio of the sown area of arable land to the total arable land area. Tabular descriptive statistics for each of these indicators are provided in Table 8.

Table 8. Descriptive statistics of variables.

Targets	2010		2015		2020	
	Average Value	Standard Deviation	Average Value	Standard Deviation	Average Value	Standard Deviation
Arable Land Area Ratio	49.003	13.734	48.835	13.668	48.095	14.383
Cultivated land transfer rate	2.697	1.397	3.082	1.534	4.445	2.833
Cropland turnover rate	4.029	2.172	4.133	2.066	5.200	4.239
Arable Land Shape Index	47.397	20.822	51.002	23.116	51.246	22.509
Arable Land Density	1.925	0.840	2.176	0.865	2.102	0.777
Yield per Unit Area	7.626	1.802	7.905	2.539	8.140	2.822
Arable Land Replanting Index	1.259	0.290	1.243	0.463	1.542	0.866

Utilizing the center of gravity model along with statistical data, the coordinates of the center of gravity for cropland use pattern and cropland sustainable use efficiency indicators within the YHHRB between 2010 and 2020 were determined. Subsequent to this, an analysis of the trajectory of the center of gravity was conducted, based on which the spatial–temporal coupling relationship and associated characteristics were investigated, aiming to furnish a theoretical foundation for subsequent research. As depicted in Figure 11, the center of gravity for the sustainable use efficiency of arable land in the YHHRB experienced a northeastward shift from 2010 to 2020. The center of gravity for each indicator of the cropland use pattern exhibited the following movements: the center of gravity for the cropland area share ratio heading northwest from 2010 to 2020; the center of gravity for the cultivated land transfer rate heading northeast from 2010 to 2020; the center of gravity for the cropland turnover rate initially moving eastward from 2010 to 2015, followed by a northeastward shift from 2015 to 2020; the center of gravity for the cropland shape index migrated northwestward during 2010–2015 and southeastward from 2015 to 2020; the center of gravity for cropland density trended southeastward from 2010 to 2015 and southwestward from 2015 to 2020; the center of gravity for yield per unit area shifted southwestward from 2010 to 2015 and northwestward from 2015 to 2020; and the center of gravity for the cropland replanting index experienced a southward and north-westward shift from 2010 to 2015, followed by a further north-westward movement from 2015 to 2020.

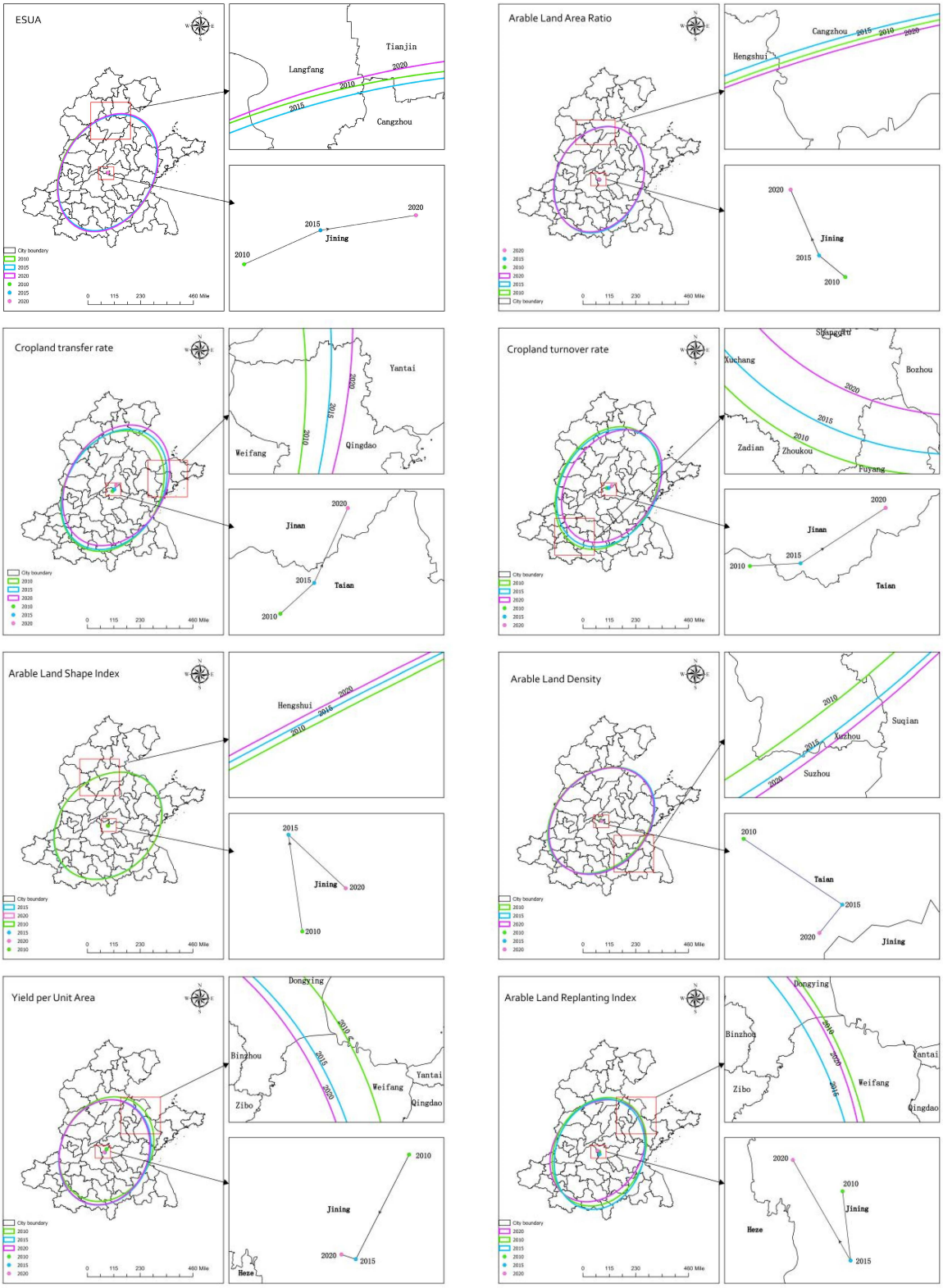

Figure 11. Migration of the center of gravity of the variables of sustainable use efficiency of arable land and arable land use pattern.

The trajectory of the center of gravity for the sustainable use efficiency of arable land aligns in the north–south direction with that of the arable land area share ratio, the arable land conversion rate, and the arable land abandonment rate, while it diverges from the direction of the arable land density and the yield per unit area in the north–south direction.

Similarly, in the east–west direction, the center of gravity for sustainable use efficiency is aligned with the movement of the arable land area share ratio and the arable land abandonment rate, whereas it exhibits a different trend from the arable land density, the yield per unit area, and the replanting index. During the period from 2010 to 2015, the center of gravity for sustainable use efficiency and the arable land shape index moved in the same direction in the north–south direction, whereas in the subsequent period from 2015 to 2020, they exhibited a similar movement in the east–west direction. In contrast, the relationship between the sustainable use efficiency of arable land and the arable land density was inverse in the north–south direction from 2010 to 2020, and they moved in the same direction in the east–west direction from 2010 to 2015. These observations suggest that there are certain correlations between the cultivated land transfer rate, conversion rate, yield per unit area, and replanting index and the efficiency of sustainable arable land use. However, the specific influence of the arable land area ratio, shape index, and density on sustainable arable land use efficiency is not yet fully understood. To delve deeper into the specific impacts of these variables on sustainable arable land use efficiency, further empirical research is warranted.

3.4. Empirical Study on Analyzing the Impact of Changes in Cropland Use Patterns on the Sustainable Use Efficiency of Cropland

In the course of assessing the stability of the selected indicators, we employed the Augmented Dickey–Fuller (ADF) unit root test to gauge the stationarity of the efficiency of sustainable arable land use, the proportion of arable land area, the rate of conversion of arable land into other uses, the rate of abandonment of arable land, the shape index of arable land, the density of arable land patches, the yield per unit area, and the replanting index. The findings reveal that all these indicators exhibit stationary characteristics, thereby refuting the conjecture of the presence of a unit root. To ascertain whether these indicators are interconnected in a long-term equilibrium, we conducted the Engle–Granger cointegration test. Initially, we hypothesized the absence of a cointegration relationship, but the *p*-value of the test result was below the 0.05 significance level, thereby warranting the rejection of the null hypothesis and affirming the presence of a cointegration relationship among these indicators. Consequently, we are justified in conducting a comprehensive analysis of these indicators using a panel data model.

Regarding the selection of a panel data model, researchers commonly confront three primary alternatives: the pooled ordinary least squares (OLS) model, the fixed effects (FE) model, and the random effects (RE) model. To discern the most fitting model, this study engaged in a comparative assessment utilizing the F-test, the Breusch–Pagan (BP) test, and the Hausman test. The outcomes disclosed *p*-values significantly below 0.05, affirming that the FE model is the most suitable choice. Additionally, the study included time as a dummy variable in the OLS regression model, and it was discerned that both the time term and the ESUA of arable land were statistically significant, indicating that temporal dynamics must be considered in the analysis. The regression outcomes for the fixed effects model that omitted the time effect were not significant, hence necessitating the establishment of a model with a time fixed effect.

Building upon the preceding analyses, we employed a time fixed effect (FE) model to examine the repercussions of alterations in cropland use patterns on the sustainable use efficiency of cropland. The regression analysis of the efficiency of sustainable arable land use within the YHHRB, alongside each variable, revealed *p*-values for the F-statistic values that were less than 0.05, corroborating the statistical significance of the regression outcomes (refer to Table 9). Among the variables, the replanting index and the cropland density demonstrated significant positive impacts on the sustainable use index of cropland, with regression coefficients of 0.138 and 0.067, respectively. This implies that for every incremental unit rise in the replanting index, the sustainable use efficiency of cropland escalates by 13.8%, and for every incremental unit increase in cropland density, it increases by 6.7%. These findings suggest that both the cropland replanting index and density have

been on the rise from 2010 to 2020, which collectively contribute to the rational utilization of land resources and the enhancement of agricultural productivity, thereby bolstering the sustainable use efficiency of cropland. In contrast, the output per unit area and the cropland transfer rate exhibited significant negative impacts, with regression coefficients of −0.02 and −0.01, respectively. This suggests that for every incremental unit increase in the output per unit area, the sustainable use efficiency of cropland decreases by 2%, and for every incremental unit rise in the cropland transfer rate, it decreases by 1%. These outcomes indicate that the escalation in unit area production and the augmentation of cropland transfer rates exert an intensifying pressure on land resources, thereby hindering the advancement of cropland ESUA. Variables such as the changes in arable land area per unit, the cultivated land transfer rate, and the shape index of arable land manifested negative effects, albeit to a lesser extent and not statistically significant. This suggests that the fluctuations in these metrics do not significantly influence the sustainable use efficiency of arable land. This might be attributable to the relatively minor magnitude of their changes or the influence of other factors, rendering their roles in improving the sustainable use efficiency of arable land less conspicuous. Consequently, these variables are not elaborated upon further in this study.

Table 9. Time fixed effects model regression results.

Variant	Ratio	t-Value	Standard Error
Intercept	1.038 ***	7.444	0.139
Arable Land Area Ratio	−0.003	−1.646	0.002
Cultivated land transfer rate	−0.02 *	−1.649	0.012
Cropland turnover rate	0.138 **	2.394	0.058
Arable Land Shape Index	−0.01 **	−2.235	0.004
Arable Land Density	−0.002	−0.593	0.003
Yield per Unit Area	−0.001	−1.342	0.001
Arable Land Replanting Index	0.067 ***	3.017	0.022

Note: *, ** and *** denote significant at the 10%, 5% and 1% statistical levels, respectively.

4. Discussion

Analysis of the quantitative disparities in the spatial distribution of arable land transfers within the study area reveals distinct patterns. The influx of arable land into the region is notably concentrated in the western mountainous and central hilly zones, whereas in the plain regions, conversion of arable land to other land uses, particularly for construction, is prevalent. This trend reflects a marked preference for "gradual encroachment to offset ruggedness", "territorial expansion to counteract elevation", and "unified occupation to nullify absence", suggesting that human influence on arable land usage is pronounced, especially in flat areas. Notably, in the plains, the encroachment of arable land by construction expansion is particularly significant [56]. Furthermore, the shift in arable land use demonstrates an adaptive response to topographical features and resource allocation, with a significant portion of arable land in Anhui and Jiangsu provinces being reallocated from water bodies. This phenomenon underscores the rapid pace of population growth and urbanization, coupled with escalating demands for land resources. To satisfy the needs of food production and economic advancement, some water-covered areas may be reclaimed for agricultural use [57]. Currently, the Jiangsu provincial government is actively promoting the policy of "converting ploughs to lakes and grasses", signaling a heightened emphasis on ecological environmental conservation and the implementation of measures to curtail the overexploitation and irrational utilization of land resources [58].

During the research period, ESUA decreased in the YHHRB. This may have been due to rapid urban development, which led to environmental pollution and agricultural structure imbalances. This developmental mindset has led to a decline in arable land quality and ecological and environmental crises [59]. Some studies have shown that the overall ESUA is higher in the YHHRB compared with other regions. However, the ESUA

trends differed among the provinces in the region (Figure 12), reflecting the different arable land conditions and local development paths. Surprisingly, the ESUAs of Henan (Yu), Shandong (Lu), and Jiangsu (Su), which form the major grain-producing area in the country ('Yulu-Suzhou'), were not high. Yulu-Suzhou is located in the Central Plains and is the country's main food production region; however, the quality of arable land has declined owing to agricultural overuse and environmental pollution. Simultaneously, owing to excessive abstraction of groundwater, the overall lack of surface water has decreased the soil water content and fertility, leading to a decrease in grain production. In 2007, with the release of the National Medium and Long-Term Urbanization Plan (2007–2020), the Yulu-Suzhou region began the process of accelerated urbanization and economic/industrial development while attracting many laborers and rapid development of secondary and tertiary industries. This resulted in serious environmental pollution and a decline in the quality and quantity of arable land [60].

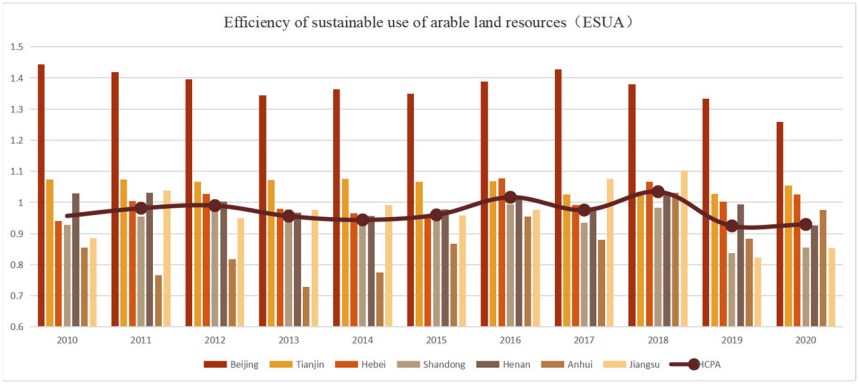

Figure 12. ESUA trends by province in the YHHRB.

The cities with the highest outputs are mainly concentrated in the provinces of Yu, Lu, and Su, which contain cities with the lowest efficiency. ESUAs are determined by desired outputs; however, inputs and undesirable outputs are also important influencing factors. Therefore, we considered not only the relationship between inputs and desired outputs but also the relationship between desired and undesired outputs, and the relationship between inputs and undesired outputs. Accordingly, we suggest two possible causes of low ESUA: (1) more non-desired outputs than desired outputs and (2) increased non-desired outputs due to input overload. The first results in low ESUA of arable land; for the second, we found that economic inputs, social inputs, ecological inputs, and non-desired outputs showed an increasing fluctuating trend in the main grain producing areas of the YHHRB during the study period; the overall growth rate was lower than the non-desired outputs, although the desired outputs also increased (Figure 13). Although the desired outputs also increased, the overall growth rate was lower than the non-desired outputs. During 2019~2020, ecological inputs, social inputs, and non-desired outputs showed a decreasing trend, while economic inputs showed an increasing trend. Therefore, the relationship between input and output factors requires further observation in future works.

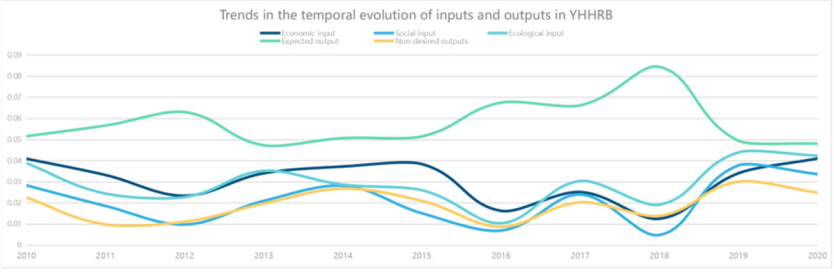

Figure 13. Temporal evolution of input–output in the YHHRB.

5. Conclusions

In this scholarly endeavor, we have developed a comprehensive evaluation index system for Sustainable Utilization of Arable Land (SUA). By integrating the Data Envelopment Analysis–Super-SBM (DGA–Super-SBM) model, the Malmquist–Luenberger production index, and the TO–Fisher–OSM algorithm, we have established a computational framework capable of handling long-time-series, high-dimensional index systems. This framework was subsequently applied to assess the Environmental Sustainable Assessments (ESUAs) for 52 prefecture-level municipalities within China's Huanghuai-Haihai Sea grain-producing regions. Our analysis delved into the trajectory of cropland use changes and the impact of these variables on ESUA. The findings of our study are as follows.

Between 2010 and 2020, the utilization of arable land within the YHHRB underwent minimal alteration, with approximately 90% of the land maintaining its agricultural status. The predominant direction of arable land conversion was to construction purposes, with the primary sources of such transfers being grasslands and aquatic systems. A spatial analysis of these patterns revealed that the conversion of arable land to construction land comprised 70.61% of the total area transferred, principally occurring in Anhui Province, Hebei Province, and the Municipality of Tianjin. Conversely, the reallocation of land from grasslands to arable land represented 35.59% of the transferred area, clustered predominantly in the western reaches of Hebei Province, the central and southern districts of Shandong Province, and the western portion of Henan Province. Additionally, the transformation of arable land from water systems to agricultural use was primarily concentrated in the eastern and southern sectors of Jiangsu Province, the central area of Tianjin Municipality, and the southeastern portion of Anhui Province.

Between the years 2010 and 2020, the Environmental Sustainable Assessment (ESUA) within the YHHRB exhibited a fluctuating trend, reaching its zenith in 2016. Geographically, ESUA progressively augmented from the west to the east, manifesting distinct spatial clustering, with a preponderance of high efficiency in the northeastern quadrant and lower levels in the southwestern reaches. The northern regions maintained their proficiency in ESUA, while the disparity between the central and northern regions lessened, and there was a marked uptick in the southern areas. The Malmquist–Luenberger production index disclosed a general decline in declining ESUA (D-ESUA), with an average annual diminution of 2.3%. However, D-ESUA increased in half of the municipalities, suggesting a transient enhancement in arable land utilization efficiency. The most substantial upsurge in D-ESUA was observed in the northern regions, at 3.2%, with more modest, fluctuating increments in the central southern parts of the country. Collectively, the sustainability of cropland resources in the Yellow and Huaihai regions is commendable.

Utilizing the center of gravity model, it was discovered that the alterations in the ESUA of arable land aligned with the north–south migration of the share of arable land area, as well as the rates of arable land conversion in and out. Conversely, these changes diverged from the movement of arable land density and the yield per unit area. In terms of the east–west progression, the gravitation of sustainable cropland use efficiency aligned with the rates of arable land conversion in and out, whereas it diverged from the trends in arable land area share, yield per unit area, and the replanting index of cropland. A time fixed effects model analysis revealed that the replanting index and cropland density exerted significant positive influences on ESUA. Conversely, the yield per unit area and the cropland turn-in rate demonstrated significant negative impacts. The alterations in cropland unit area, cropland turnout rate, and cropland shape index demonstrated negative effects, albeit minor and insignificant in statistical terms.

Under the environment of accelerating the construction of a strong agricultural country and comprehensively realizing the revitalization of the countryside, SUA is an important driving force to promote green modernization of agriculture and rural areas. It is important to study the evaluation criteria and spatiotemporal evolution of SUA to clarify the direction of sustainable development of arable land, drive the development of peripheral cities by high-efficiency cities, and drive peripheral cities by the main food-producing areas to ulti-

mately achieve strategic sustainable development of arable land across the whole country. Owing to limitation of the model parameters, DGA–Super-SBM can only evaluate static sustainable utilization index systems; however, in reality, arable land changes dynamically. Therefore, it is necessary to identify dynamic indicators for the dynamic monitoring of sustainable utilization. How to evaluate high-dimensional dynamic indicator systems is a research direction for the future.

Author Contributions: Conceptualization, C.D.; methodology, Y.Z. and X.H.; validation, formal analysis, X.H.; data collation, X.H.; writing—original manuscript preparation, X.H. All authors have read and agreed to the published version of the manuscript.

Funding: This study was funded by the Project on Basic Research Operations of Central Research Institutes: Research on the Construction of Natural Resources Survey and Monitoring Technology System and Some Key Technologies (No. AR2203).

Data Availability Statement: The data presented in this study are available on request from the corresponding author due to the confidentiality of the data.

Acknowledgments: This study was made possible by the contributions and support of many parties. Please accept our apologies for any omissions. We would like to thank the institution that funded our research, the Project on Basic Research Operations of Central Research Institutes: Research on the Construction of Natural Resources Survey and Monitoring Technology System and Some Key Technologies (No. AR2203), and the editors and reviewers of Ecological Indicators for their professional comments on this manuscript. Without your contributions, our research would not have been possible. All authors agree to the content of the acknowledgements.

Conflicts of Interest: The authors declare no conflicts of interest.

References

1. Bai, Z.; Caspari, T.; Gonzalez, M.R.; Batjes, N.H.; Mader, P.; Bunemann, E.K.; de Goede, R.; Brussaard, L.; Xu, M.; Ferreira, C.S.S.; et al. Effects of agricultural management practices on soil quality: A review of long-term experiments for Europe and China. *Agric. Ecosyst. Environ.* **2018**, *265*, 1–7. [CrossRef]
2. FAO. *The 10 Elements of Agroecology: Guiding the Transition to Sustainable Food and Agricultural Systems*; Food and Agriculture Organization of the United Nations: Rome, Italy, 2018. Available online: http://www.fao.org/3/i9037en/i9037en.pdf (accessed on 10 May 2024).
3. Rajbanshi, J.; Das, S.; Paul, R. Quantification of the effects of conservation practices on surface runoff and soil erosion in croplands and their trade-off: A meta-analysis. *Sci. Total Environ.* **2023**, *864*, 161015. [CrossRef] [PubMed]
4. Long, H.; Ge, D.; Zhang, Y.; Tu, S.; Qu, Y.; Ma, L. Changing man-land interrelations in China's farming area under urbanization and its implications for food security. *J. Environ. Manag.* **2018**, *209*, 440–451. [CrossRef]
5. Wang, W.; Cao, Y.; Su, R.; Qiu, M.; Song, L.; Zhou, W. Cultivated Land Protection Policy in China: Background Effect and Future Trends. *Chin. J. Agric. Resour. Reg. Plan.* **2020**, *41*, 40–51. [CrossRef]
6. Wang, C.; Sun, X.; Wang, M.; Wang, J.; Ding, Q. Chinese Cropland Quality and Its Temporal and Spatial Changes due to Urbanization in 2000–2015. *J. Resour. Ecol.* **2019**, *10*, 174–183. [CrossRef]
7. Dai, A. Study on soil environmental protection and control strategy. *Huanjingyufazhan* **2020**, *32*, 36–37. [CrossRef]
8. Yu, Z.; Chen, C.; Cui, Z. Impacts of changes in cultivated land use patterns on total factor productivity of grain in the three northeastern provinces, China. *J. Agric. Resour. Environ.* **2024**, *41*, 1–14. [CrossRef]
9. Liu, D.; Liu, F.; Niu, W.; Hao, Z.; Sheng, K.; Zhang, B.; Wang, Z. Spatial-temporal Changes and Driving Factors of Cultivated Land Intensive Use in Inner Mongolia Autonomous Region from 1985 to 2018. *Bull. Soil Water Conserv.* **2022**, *42*, 365–372.
10. Zhao, Y.; Tan, Y. Spatial-temporal Changes of Cultivated Land Use at Provincial Level Since Second National Land Survey in China. *Bull. Soil Water Conserv.* **2020**, *40*, 204–212. [CrossRef]
11. Luo, H.; Pan, L.; Hu, X.; Liu, Z. Study on grain and ecological effects of arable land use change in major grain-producing are as in China. *Acta Agric. Zhejiangensis* **2023**, *35*, 226–237. [CrossRef]
12. Dong, Q. Analysis and Research on Land Use Change of Cultivated Land Extraction from Remote Sensing lmages of Changchun City Based on ArcGIS. Master's Thesis, Jilin Agricultural University, Jilin, China, 2022.
13. Wang, Y.-R.; Ji, M.; Guo, F.-B.; Li, Z. Study on Spatio-temporal Variation and Influencing Factors of Farmland Utilization Ecological Efficiency in Shandong Province. *Acta Agric. Jiangxi* **2023**, *35*, 130–137. [CrossRef]
14. Dong, G.; Liu, Z.; Niu, Y.; Jiang, W. Identification of Land Use Conflicts in Shandong Province from an Ecological Security Perspective. *Land* **2022**, *11*, 2196. [CrossRef]
15. Zhao, D.; Xu, C. Structural Model and Empirical Analysis of Bond Pricing in Government Implicit Guarantee. *J. Tongji Univ. Nat. Sci.* **2020**, *48*, 1506–1514. [CrossRef]

16. Gao, R.; Zhang, Z.; Li, W.; Li, M.; Niu, Y.; Zhang, R.; Zhang, G.; Yuan, L.; Zhang, C. Effects of Cultivated Land on Wind Erosion of Annual Land Use Change at Lankao County, Henan Province During 2018–2019. *Bull. Soil Water Conserv.* **2021**, *41*, 112–117+124. [CrossRef]
17. Weiland, U.; Kindler, A.; Banzhaf, E.; Ebert, A.; Reyes-Paecke, S. Indicators for sustainable land use management in Santiago de Chile. *Ecol. Indic.* **2011**, *11*, 1074–1083. [CrossRef]
18. Hurni, H. Assessing sustainable land management (SLM). *Agric. Ecosyst. Environ.* **2000**, *81*, 83–92. [CrossRef]
19. Alipbeki, O.; Alipbekova, C.; Sterenharz, A.; Toleubekova, Z.; Makenova, S.; Aliyev, M.; Mineyev, N. Analysis of Land-Use Change in Shortandy District in Terms of Sustainable Development. *Land* **2020**, *9*, 147. [CrossRef]
20. Uisso, A.M.; Tanrivermis, H. Driving factors and assessment of changes in the use of arable land in Tanzania. *Land Use Policy* **2021**, *104*, 105359. [CrossRef]
21. Zerriffi, H.; Reyes, R.; Maloney, A. Pathways to sustainable land use and food systems in Canada. *Sustain. Sci.* **2023**, *18*, 389–406. [CrossRef] [PubMed]
22. Zhang, W.; Cheng, Q.; Cha, X. Study on the Influencing Factors of Cultivated Land "Non-grain" from the Perspective of Sustainable Development. *Food Sci. Technol. Econ.* **2022**, *47*, 9–14. [CrossRef]
23. Cui, Y.; Long, Y.-L. Study on Evaluation of Sustainable Utilization of Cultivated Land Based on Structural Equation Model. *Acta Agric. Jiangxi* **2020**, *32*, 126–135. [CrossRef]
24. Liu, H.-J. Study on Sustainable Utilization of Cultivated Land in Hunan Province Based on Ecological Footprint Model. *J. Anhui Agric. Sci.* **2022**, *50*, 53–56+93. [CrossRef]
25. Potapov, P.; Turubanova, S.; Hansen, M.C.; Tyukavina, A.; Zalles, V.; Khan, A.; Song, X.-P.; Pickens, A.; Shen, Q.; Cortez, J. Global maps of cropland extent and change show accelerated cropland expansion in the twenty-first century. *Nat. Food* **2022**, *3*, 19–28. [CrossRef] [PubMed]
26. Zabel, F.; Delzeit, R.; Schneider, J.M.; Seppelt, R.; Mauser, W.; Vaclavik, T. Global impacts of future cropland expansion and intensification on agricultural markets and biodiversity. *Nat. Commun.* **2019**, *10*, 2844. [CrossRef] [PubMed]
27. Daqui, Z. *Environmental Geology*; Higher Education Press: Beijing, China, 2000.
28. Liang, X.; Jin, X.; Dou, Y.; Zhang, X.; Li, H.; Wang, S.; Meng, F.; Tan, S.; Zhou, Y. Mapping sustainability-oriented China's cropland use stability. *Comput. Electron. Agric.* **2024**, *219*, 108823. [CrossRef]
29. Wang, X.; Hao, J.-Q.; Dai, Z.-Z.; Haider, S.; Chang, S.; Zhu, Z.-Y.; Duan, J.-J.; Ren, G.-X. Spatial-temporal characteristics of cropland distribution and its landscape fragmentation in China. *Farming Syst.* **2024**, *2*, 100078. [CrossRef]
30. Folberth, C.; Khabarov, N.; Balkovič, J.; Skalský, R.; Visconti, P.; Ciais, P.; Janssens, I.A.; Peñuelas, J.; Obersteiner, M. The global cropland-sparing potential of high-yield farming. *Nat. Sustain.* **2020**, *3*, 281–289. [CrossRef]
31. Sünnemann, M.; Beugnon, R.; Breitkreuz, C.; Buscot, F.; Cesarz, S.; Jones, A.; Lehmann, A.; Lochner, A.; Orgiazzi, A.; Reitz, T.; et al. Climate change and cropland management compromise soil integrity and multifunctionality. *Commun. Earth Environ.* **2023**, *4*, 394. [CrossRef]
32. Zhang, Z.; Du, J.; Shen, Z.; El Asraoui, H.; Song, M. Effects of modern agricultural demonstration zones on cropland utilization efficiency: An empirical study based on county pilot. *J. Environ. Manag.* **2024**, *349*, 119530. [CrossRef] [PubMed]
33. Winkler, K.; Fuchs, R.; Rounsevell, M.; Herold, M. Global land use changes are four times greater than previously estimated. *Nat. Commun.* **2021**, *12*, 2501. [CrossRef] [PubMed]
34. Zheng, Y.; Long, H.; Chen, K. Spatio-temporal patterns and driving mechanism of farmland fragmentation in the Huang-Huai-Hai Plain. *J. Geogr. Sci.* **2022**, *32*, 1020–1038. [CrossRef]
35. Ge, D.; Long, H.; Li, Y.; Zhang, Y.; Tu, S. The Spatio-Temporal Pattern of Multifunctional Transformation of China's Grain Production System in the Process of Urbanization: The Case of Huang-Huai-Hai Plain. *Econ. Geogr.* **2018**, *38*, 147–156+182. [CrossRef]
36. Tone, K. A slacks-based measure of super-efficiency in data envelopment analysis. *Eur. J. Oper. Res.* **2002**, *143*, 32–41. [CrossRef]
37. Chi, M.J.; Guo, Q.Y.; Mi, L.C.; Wang, G.F.; Song, W.M. Spatial Distribution of Agricultural Eco-Efficiency and Agriculture High-Quality Development in China. *Land* **2022**, *11*, 722. [CrossRef]
38. Wei, J.X.; Lei, Y.L.; Yao, H.J.; Ge, J.P.; Wu, S.M.; Liu, L.N. Estimation and influencing factors of agricultural water efficiency in the Yellow River basin, China. *J. Clean. Prod.* **2021**, *308*, 127249. [CrossRef]
39. Lu, Z.-F.; Deng, W.M.; Zhu, W.W. Dynamic Evaluation of Ecological Environment Governance Performance of Jiangsu Province Based on PC-SBVndexano. *East China Econ. Manag.* **2019**, *33*, 32–38. [CrossRef]
40. Pishgar-Komleh, S.H.; Cechura, L.; Kuzmenko, E. Investigating the dynamic eco-efficiency in agriculture sector of the European Union countries. *Environ. Sci. Pollut. Res.* **2021**, *28*, 48942–48954. [CrossRef] [PubMed]
41. Caves, D.W.; Christensen, L.R.; Diewert, W.E. The Economic-Theory of Index Numbers and the Measurement of Input, Output, and Productivity. *Econometrica* **1982**, *50*, 1393–1414. [CrossRef]
42. Aparicio, J.; Santin, D. A note on measuring group performance over time with pseudo-panels. *Eur. J. Oper. Res.* **2018**, *267*, 227–235. [CrossRef]
43. Pastor, J.T.; Lovell, C.A.K.; Aparicio, J. Defining a new graph inefficiency measure for the proportional directional distance function and introducing a new Malmquist productivity index. *Eur. J. Oper. Res.* **2020**, *281*, 222–230. [CrossRef]
44. Pan, W.-T.; Zhuang, M.-E.; Zhou, Y.-Y.; Yang, J.-J. Research on sustainable development and efficiency of China's E-Agriculture based on a data envelopment analysis-Malmquist model. *Technol. Forecast. Soc. Chang.* **2021**, *162*, 120298. [CrossRef]

45. Gosme, M.; Suffert, F.; Jeuffroy, M.H. Intensive versus low-input cropping systems: What is the optimal partitioning of agricultural area in order to reduce pesticide use while maintaining productivity? *Agric. Syst.* **2010**, *103*, 110–116. [CrossRef]
46. Mobe, N.T.; Dzikiti, S.; Dube, T.; Mazvimavi, D.; Ntshidi, Z. Modelling water utilization patterns in apple orchards with varying canopy sizes and different growth stages in semi-arid environments. *Sci. Hortic.* **2021**, *283*, 110051. [CrossRef]
47. Qin, N. Prediction of cultivated land dem and based on Fisher arithmetic and Markov Chamn Model with Weights—A case study of Liao Cheng city. *Sci. Surv. Mapp.* **2011**, *36*, 29–31. [CrossRef]
48. Wang, J.X.; Wang, X.R.; Zhou, S.L.; Wu, S.H.; Zhu, Y.; Lu, C.F. Optimization of Sample Points for Monitoring Arable Land Quality by Simulated Annealing while Considering Spatial Variations. *Int. J. Environ. Res. Public Health* **2016**, *13*, 980. [CrossRef] [PubMed]
49. Song, C.; Wu, B.; Zhao, J.; Xu, Z. An integrated output space partition and optimal control method of multiple-model for nonlinear systems. *Comput. Chem. Eng.* **2018**, *113*, 32–43. [CrossRef]
50. Dinakaran, K.; Rajalakshmi, D.; Valarmathie, P. Efficient pattern matching for uncertain time series data with optimal sampling and dimensionality reduction. *Microprocess. Microsyst.* **2020**, *75*, 103057. [CrossRef]
51. Lyu, X.; Sun, X.; Peng, W.; Niu, S. Spatial-Temporal Differentiation of Sustainable Intensification of Cultivated Land Use in Shenyang City Based on Emergy Analysis. *China Land Sci.* **2022**, *36*, 79–89. [CrossRef]
52. Gong, Y.; Li, J.; Li, Y. Spatiotemporal characteristics and driving mechanisms of arable land in the Beijing-Tianjin-Hebei region during 1990–2015. *Socio-Econ. Plan. Sci.* **2020**, *70*, 100720. [CrossRef]
53. Huang, H.; Wen, L.; Kong, X.; Chen, W.; Sun, X. The Impact of Spatial Pattern Evolution of Cultivated Land on Cultivated Land Suitability in China and Its Policy Implication. *China Land Sci.* **2021**, *35*, 61–70. [CrossRef]
54. Jiao, X.-Q.; Mongol, N.; Zhang, F.-S. The transformation of agriculture in China: Looking back and looking forward. *J. Integr. Agric.* **2018**, *17*, 755–764. [CrossRef]
55. Sun, Y.; Wang, N. Sustainable urban development of the pi-shaped Curve Area in the Yellow River basin under ecological constraints: A study based on the improved ecological footprint model. *J. Clean. Prod.* **2022**, *337*, 130452. [CrossRef]
56. Kuang, W.; Zhang, S.; Du, G. Remotely sensed mapping and analysis of spatio-temporal patterns of land use change across China in 2015–2020. *Acta Geogr. Sin.* **2022**, *77*, 1056–1071. [CrossRef]
57. Lu, D.; Wang, Z.; Su, K.; Zhou, Y.; Li, X.; Lin, A. Understanding the impact of cultivated land-use changes on China's grain production potential and policy implications: A perspective of non-agriculturalization, non-grainization, and marginalization. *J. Clean. Prod.* **2024**, *436*, 140647. [CrossRef]
58. Gao, C.; Luo, Y.; Li, P. Does the Regional Ecological Security Pattern Benefit Eco-Environmental Protection? A Case Study of Yangtze River Delta. *Ecosyst. Health Sustain.* **2023**, *9*, 0017. [CrossRef]
59. Hou, Y.; Chen, Y.; Li, Z.; Wang, Y. Changes in Land Use Pattern and Structure under the Rapid Urbanization of the Tarim River Basin. *Land* **2023**, *12*, 693. [CrossRef]
60. Yin, G.; Lin, Z.; Jiang, X.; Yan, H.; Wang, X. Spatiotemporal differentiations of arable land use intensity—A comparative study of two typical grain producing regions in northern and southern China. *J. Clean. Prod.* **2019**, *208*, 1159–1170. [CrossRef]